jove

Thermochemical Studies of Ni(II) and Zn(II) Ternary Complexes using Ion Mobility-Mass Spectrometry

Anna J. Corrales[1], **Anna V. Arredondo**[1], **Amber A. Flores**[1], **Chloe L. Duvak**[1], **Charles L. Mitchell**[1], **Riccardo Spezia**[2], **Laurence A. Angel**[1]

[1] Department of Chemistry, Texas A&M University-Commerce [2] Laboratoire de Chimie Théorique, Sorbonne Université

Corresponding Author

Laurence A. Angel
laurence.angel@tamuc.edu

Citation

Corrales, A.J., Arredondo, A.V., Flores, A.A., Duvak, C.L., Mitchell, C.L., Spezia, R., Angel, L.A. Thermochemical Studies of Ni(II) and Zn(II) Ternary Complexes using Ion Mobility-Mass Spectrometry. *J. Vis. Exp.* (184), e63722, doi:10.3791/63722 (2022).

Date Published

June 8, 2022

DOI

10.3791/63722

URL

jove.com/video/63722

Abstract

This article describes an experimental protocol using electrospray-ion mobility-mass spectrometry (ES-IM-MS) and energy-resolved threshold collision-induced dissociation (TCID) to measure the thermochemistry of the dissociation of negatively-charged [amb+M(II)+NTA]$^-$ ternary complexes into two product channels: [amb+M(II)] + NTA or [NTA+M(II)]$^-$ + amb, where M = Zn or Ni and NTA is nitrilotriacetic acid. The complexes contain one of the alternative metal binding (amb) heptapeptides with the primary structures acetyl-His_1-Cys_2-Gly_3-Pro_4-Tyr_5-His_6-Cys_7 or acetyl-Asp_1-Cys_2-Gly_3-Pro_4-Tyr_5-His_6-Cys_7, where the amino acids' $Aa_{1,2,6,7}$ positions are the potential metal-binding sites. Geometry-optimized stationary states of the ternary complexes and their products were selected from quantum chemistry calculations (presently the PM6 semi-empirical Hamiltonian) by comparing their electronic energies and their collision cross-sections (CCS) to those measured by ES-IM-MS. From the PM6 frequency calculations, the molecular parameters of the ternary complex and its products model the energy-dependent intensities of the two product channels using a competitive TCID method to determine the threshold energies of the reactions that relate to the 0 K enthalpies of dissociation (ΔH_0). Statistical mechanics thermal and entropy corrections using the PM6 rotational and vibrational frequencies provide the 298 K enthalpies of dissociation (ΔH_{298}). These methods describe an EI-IM-MS routine that can determine thermochemistry and equilibrium constants for a range of ternary metal ion complexes.

Introduction

This study describes a new technique using a commercially available ion mobility-mass spectrometer that allows the determination of the relative thermochemistry for the dissociation of an alternative metal binding (amb) ternary metal complex [amb+M(II)+NTA], where M = Zn or Ni and NTA = nitrilotriacetic acid (**Figure 1**). These reactions model

the dissociation of the amb-tagged recombinant protein attached to the NTA-immobilized metal during immobilized metal affinity chromatography (IMAC)[1,2]. As an example, this method is described using the amb heptapeptide tags of amb **A** and **H** (**Figure 2**) (chosen from the previous studies[3,4,5,6,7,8,9,10,11,12]) that exhibit Zn(II) and Ni(II)-binding properties and, thus, have potential applications as purification tags. However, the described process can be used to evaluate thermochemical energies in any organometallic system. These amb peptides have metal-binding sites in the Aa_1-Aa_2 and Aa_6-Aa_7 positions that compete with the carboxylate and amine sites of the NTA. The three central amb amino acids provide a spacer (Gly_3), the hinge for the two arms (Pro_4), and a long-distance π-metal cation interaction (Tyr_5).

The overall 1− charge state of the $[amb+M(II)+NTA]^-$ complexes is determined by the protonation state of their potential binding sites. Since there is Ni(II) or Zn(II) with the 2+ oxidation state, there must be a net of three deprotonated negatively-charged sites. The molecular modeling of the $[amb+M(II)+NTA]^-$ complexes predicts that these are two protons from the NTA and one proton from the amb (i.e., $[amb-H+M(II)+NTA-2H]^-$). The product channels contain an ionic species and a neutral species (i.e., $[NTA-3H+M(II)]^-$ + amb or $[amb-3H+M(II)]^-$ + NTA). In the manuscript, "-3H" is excluded in the names of the complexes, but the reader should know that the -3H is implied. The instrument measures the relative intensities of the two ionic mass-to-charge (*m/z*) species. A major attribute of ES-IM-MS analyses is that it allows the examination of the reactivity of a specific *m/z* species, as utilized here and in previous amb studies[3,4,5,6,7,8,9,10,11,12].

Acquiring thermochemical data for large complexes using collision-induced dissociation is a subject of significant interest[13,14]. Methodologies including the kinetic method are not conducive to fitting data over a range of energies, nor do they account for multi-collision environments[15,16,17,18]. Here, the threshold CID (TCID) method, developed using guided ion beam tandem mass spectrometry by Armentrout, Ervin, and Rodgers is applied[19] to a new ES-IM-MS instrument platform utilizing traveling-wave ion guides. The TCID method allows for relative thermochemical analysis of the dissociation of the ternary complexes into their two product channels and includes a threshold law describing the transfer of collision energy between the translational energy of the reactant (ternary complex in this research) and an inert target gas (argon in this case). The method includes integration over the reactant's internal energy distribution[20], the translational energy distributions between the reactant and target gas[21], and the total angular momentum distributions[22,23]. A dissociation probability and statistical Rice-Ramsperger-Kassel-Marcus (RRKM) correction of the kinetic shifts resulting from the limited time window for observation of the products are included[24]. For two independent product channels, the competitive TCID method allows for the simultaneous fitting of the two competing product channels. Dissociation of the complex is through an orbiting transition state, which has the properties of the products but is held together by a locked-dipole[25]. The TCID method is incorporated into the CRUNCH program[26], and the operation of the user interface is described here to evaluate the thermochemistry of the two dissociation channels of the ternary $[amb+M(II)+NTA]^-$ complexes. The CRUNCH program is available upon request from the developers[26].

Protocol

NOTE: **Figure 1** shows an overview of the protocol.

1. Preparation of reagents

1. Purchase freeze-dried amb peptides (>98% purity) and store them in a −80 °C freezer.
2. Purchase >99% purity zinc(II) nitrate hexahydrate and nickel(II) nitrate hexahydrate.
   CAUTION: Nickel(II) nitrate hexahydrate presents an environmental and health hazard.
3. Purchase the nitrilotriacetic acid, poly-DL-alanine polymers, ultrapure/trace metal grade ammonium acetate, ammonium hydroxide, glacial acetic acid, and HPLC grade acetonitrile.

2. Preparation of stock solutions

1. Peptide amb stock solution
   1. Prepare an aqueous solution of 12.5 mM amb concentration by weighing 10-20 mg of the freeze-dried peptide using no less than three significant figures and placing it in a 1.7 mL polypropylene microcentrifuge tube.
   2. Add the appropriate volume of deionized water (>17.8 MΩ cm) to the microcentrifuge tube. Close the lid and mix well with at least 20 inversions.
   3. Create 50 µL aliquots from the 12.5 mM amb solution and place them into marked 1.7 mL microcentrifuge tubes. Store the aliquot stock solutions at −80 °C.
2. Metal ion stock solutions
   1. Prepare the aqueous Zn(II) and Ni(II) solutions of 12.5 mM concentration by weighing 10-30 mg of the metal nitrate hexahydrate using no less than three significant figures and placing it in a 1.7 mL polypropylene microcentrifuge tube.
   2. Add the appropriate amount of DI water to the microcentrifuge tube. Close the lid and mix well with at least 20 inversions. Store 50 µL aliquot stock solutions at −80 °C.
3. NTA ion stock solutions
   1. Prepare an aqueous NTA solution by weighing 10-30 mg of the NTA using no less than three significant figures and placing it in a 1.7 mL microcentrifuge tube.
   2. Add the appropriate amount of DI water to the NTA in the microcentrifuge tube to achieve a final concentration of 12.5 mM. Close the lid and mix well with at least 20 inversions. Store 50 µL aliquot stock solutions at −80 °C.
4. Ammonium acetate stock solutions: Weigh 30.8 mg of ammonium acetate and add to 40 mL of DI water to yield a 10 mM solution. Adjust the pH of the ammonium acetate solution to pH 7.7 with 1 mM ammonium hydroxide.
5. Poly-DL-alanine stock solution: Make a 1 mL, 1,000 ppm poly-DL-alanine (PA) stock solution by dissolving 1.0 mg of PA in DI water. Mix comprehensively. Create 50 µL aliquots and put them into individually labeled microcentrifuge tubes. Store the 1,000 ppm solution at −80 °C.

3. Electrospray-ion mobility-mass spectrometry (ES-IM-MS) collision-induced dissociation (CID) analysis

1. Prepare the instrument by cleaning the ES inlet tubing and metal capillary by injecting 500 µL of 0.1 M glacial acetic acid, followed by 500 µL of 0.1 M ammonium hydroxide, and finally 500 µL of pH 7.7 ammonium acetate solution.
2. Liquefy the 12.5 mM amb stock solution by bringing it to room temperature. Create a final concentration of 0.125 mM amb by making two successive dilutions with DI water. Mix comprehensively after each dilution.
3. Liquefy the 12.5 mM metal ion stock solution by bringing it to room temperature. Create a final concentration of 0.125 mM metal ion by making two successive dilutions with DI water. Mix comprehensively after each dilution.
4. Liquefy the 12.5 mM NTA stock solution. Create a final concentration of 0.125 mM NTA by making two successive dilutions with DI water. Mix comprehensively after each dilution.
5. To make a 2 mL sample of the ternary complex, add 800 µL of 0.125 mM NTA solution and 400 µL of 0.125 metal ion solution to a 2 mL microcentrifuge tube, and mix thoroughly with at least 20 inversions. Add 400 µL of ammonium acetate solution (pH 7.7) and 400 µL of 0.125 mM amb solution, mix thoroughly with at least 20 inversions, and permit the sample to equilibrate for 10 min at room temperature.
6. Load the 2 mL sample into a 2.5 mL blunt nose syringe and inject the sample into the ES of the instrument using the instrument's syringe pump at a flow of 10 µL/min.
7. Place the instrument in negative IM-MS mode. Use the typical operating conditions of the instrument[27] for these experiments as follows.
    1. Inject the sample at a 10 µL/min flow rate into the ES capillary held at −2 kV with a 500 L/h desolvation flow rate of nitrogen. Set the ES source and desolvation temperatures to 130 °C and 263 °C, respectively. Set the sampling and extraction cones to 25 V and 3 V, respectively.
    2. For the CID experiments, use the quadrupole mass analyzer to select the isotopic pattern of the [amb +M(II)+NTA]$^-$ ternary complex using the *m/z* of the monoisotopic peak with resolution settings of low mass = 4.5 and high mass = 16.5.

        NOTE: The [amb+M(II)+NTA]$^-$ ions are passed onto the sequential three traveling wave (T-wave) ion guides.
    3. Ensure that the trap T-wave has an argon gas flow of 3 mL/min and a pressure of 2.83 x 10^{-2} mbar. Set the collision energy (CE) to the trap at 5 V to avoid any dissociation of the ternary complex. Let the trap collect the ternary complex ions before releasing (200 µs release time) them into the ion mobility (IM) T-wave ion guide using a trap DC bias of 14 V, which keeps dissociation of the complex at the IM entrance to a minimum.
    4. Ensure that the IM ion guide has a pressure of 0.507 mbar using a 20 mL/min flow rate of ultrapure N_2 buffer gas. Ramp the T-waves in the IM with heights of 7 V to 30 V and with velocities of 290 m/s to 801 m/s for each starting and ending sweep of the IM ion guide.

5. Set the argon flow and pressure of the transfer T-wave the same as the trap T-wave. The transfer T-wave was used for the collision-induced dissociation of the ternary [amb+M(II)+NTA]$^-$ complex using the transfer CE.

8. Select the *m/z* isotope pattern of the negatively charged [amb+M(II)+NTA]$^-$ complex using the transmission quadrupole in resolving mode.

1. Identify the *m/z* isotope pattern by opening the mass spectrometry program and selecting **Spectrum**. Select **Tools > Isotope model**. In the pop-up window, list the molecular formula of the complex, check the box for **Show Charged Ion**, enter 1 for the charge of negative one and click on **OK**.

2. In the displayed isotope pattern of the complex, note the lowest mass peak. In the instrument software, select **Setup > Quad Profile**. In the window that opens, select **Manual Fixed** and enter the mass of the lowest isotopic pattern peak. Click on **Update** and then **Close**.

3. Select **Setup** again, and then click on **Resolving Quad**. Collect the negative ion ES-IM-MS spectra incrementally across a range of transfer collision energies using a 5 min run duration and 2 s scan time.

NOTE: Preliminary transfer energies can be tested from 26-60 V in intervals of 2 V. The final range of transfer collision energies examined should demonstrate no dissociation of the ternary complex at the lowest energy and complete dissociation into the products at the highest energy. For high-quality statistical analysis, this ES-IM-MS analysis should be performed for each amb ternary complex at least 3x by different people and on different days to determine means and standard deviations.

4. ES-IM-MS collision cross-section (CCS) analysis

1. Clean the ES inlet tubing and the metal capillary with 500 µL of 0.1 M glacial acetic acid, followed by 500 µL of 0.1 M ammonium hydroxide, and finally 500 µL of pH 7.7 ammonium acetate solution.

2. Liquefy the 1,000 ppm PA stock solution to room temperature and do two serial dilutions; dilute to 100 ppm PA with DI water, and then dilute to 10 ppm PA solution by diluting with a 1:1 ratio of DI water and HPLC-grade acetonitrile.

3. Collect the negative ion IM-MS spectra of the 10 ppm PA sample for 10 min using instrumental operating conditions.

NOTE: The injection flow rate and ES source conditions were the same as for the CID experiments (step 3.). For measurements of the CCS, the quadrupole mass analyzer was in non-resolving mode and passed all ions onto the sequential three T-wave ion guides. The operation of the trap T-wave and IM T-wave ion guides was the same as for the CID experiments. The collision energy of the transfer T-wave cell was at 4 V to allow ions to pass through without dissociation.

4. Prepare each of the ternary complexes as described in steps 3.2.-3.6.

5. Collect the IM-MS spectra of each ternary complex for 5 min.

NOTE: Use the same instrumental conditions as in step 4.3.

6. Collect the negative ion IM-MS spectra of the 10 ppm PA sample for 10 min.

   NOTE: The mean of the arrival times of the PA calibrants collected before and after the amb ternary complexes are used in the CCS determination.

5. Analysis of ES-IM-MS CID data

1. Identify the species by matching the theoretical *m/z* isotope patterns of the ternary complex and its products to the experimental IM-MS spectra.
   1. Open the mass spectrometry program and select **Chromatogram** to open a new window.
   2. In the **Chromatogram** window, click on **File > Open** to find and open the desired IM-MS data file.
   3. Right-clicking the mouse, drag across the chromatogram, and release. The MS spectrum will be displayed in a separate **Spectrum** window.
   4. In the new window displaying the spectra, select **Tools > Isotope Model**. A small window will pop up. Enter the molecular formula of the amb species, check the **Show Charged Ion** box, and enter the desired charge state. Click on **OK**.
   5. To distinguish all the species in the IM-MS spectrum, repeat this process in the **Spectrum** window and record their *m/z* isotope range.
2. For the ternary amb complex and its products, use their *m/z* isotope range to identify them and extract their arrival time distributions (ATD).
   1. Open the ion mobility separation software and select **File > Open** to find and open the data file.
   2. Left-click and drag with the mouse to zoom in on the *m/z* isotope range of the ternary complex [amb +M(II)+NTA]$^-$.
   3. Using the **Selection** tool, left-click and drag to select the specific isotope range for [amb+M(II)+NTA]$^-$ as identified in step 5.1. Click on the **Accept Current Selection** button.
   4. To eliminate any coincidental *m/z* species or background signal, use the **Selection** tool to choose the ATD associated with the ternary complex. Click on the **Accept Current Selection** button.
   5. To export the ATD file to the mass spectrometry software, go to **File > Export**, and then click on **Retain Drift Time**. Rename the file if desired and save the file in the appropriate folder.
3. Determine by integration of the area under the extracted ATD curve the species' relative intensity.
   1. In the **Chromatogram** window, open the saved exported file from the ion mobility separation software. Select **Process** and then **Integrate**. Use a peak-to-peak amplitude setting of 20 and click on **OK**.
   2. Record the integrated area as shown on the **Chromatogram** window. Repeat steps 5.2.2.-5.2.5. for the two products, namely [NTA+M(II)]$^-$ and [amb +M(II)]$^-$.
   3. Repeat steps 5.2.1.-5.3.2. for each transfer collision energy recorded.
4. Utilize the integrated ATD areas for the ternary complex [amb+M(II)+NTA]$^-$ and two products [NTA+M(II)]$^-$ and

[amb+M(II)]$^-$ at each transfer collision energy point to normalize to a relative percentage scale.

1. Create a spreadsheet by entering the identities of the ternary complex and its products and their integrated ATD at each collision energy.
2. For each collision energy, utilize the summation of the integrated ATDs for [amb+M(II)+NTA]$^-$, [NTA+M(II)]$^-$, and [amb+M(II)]$^-$ to normalize their individual ATDs to a relative percentage scale.
3. From the replicate TCID measurements, find the mean and standard deviations of each data point. Convert the lab-frame transfer collision energy (E_{lab}) to the center-of-mass collision energy (E_{cm}) using the average masses of the argon (m_{Ar}) collision gas and the ternary complex ($m_{complex}$): $E_{cm} = E_{lab}\ (m_{Ar})/(m_{Ar} + m_{complex})$.
   NOTE: E_{cm} represents the maximum energy from the collision with the argon gas, which is available for dissociation of the ternary complex.
4. Plot the mean and standard deviation of the individual percentage intensities of [amb +M(II)+NTA]$^-$, [NTA+M(II)]$^-$, and [amb+M(II)]$^-$ in a graph of relative intensity (%) vs. center-of-mass collision energy (eV) to exhibit how the species' relative intensities change as a function of collision energy.

6. Analysis of the average arrival times for determining collision cross-sections (CCS)

1. Open the ion mobility separation software and the file containing the IM-MS spectrum of the 10 ppm PA sample collected with the transfer collision energy set at 4 V. Extract the ATD of each of the single negatively charged PA species and export the files to the mass spectrometry software using the option **Retain Drift Time** (see step 5.2.5.). Repeat for the second PA calibrants file.
2. Open the ion mobility separation software. Use **File > Open** to open one of the files containing the IM-MS spectra of the amb ternary complexes recorded between the PA calibrants. Extract the ATD of each of the ternary complexes and export their files to the mass spectrometry software using the **Retain Drift Time** option (see step 5.2.5.).
3. Use a cross-sectional calibration method[28] to calculate the CCS of the ternary complex and its products.
   1. In a spreadsheet, calculate the corrected CCS (Ω_c) for each of the single negatively charged PA species from their CCS (Ω)[29,30] measured in Helium buffer gas[31] using **Equation 1**, where z = charge of the ternary complex, e_c = 1.602 x 10^{-19} C; m_{N2} = mass of nitrogen (u), and m_{ion} = mass of ternary complex[28].

$$\Omega_c = \frac{\Omega}{ze_c\sqrt{\left(\frac{1}{m_{N_2}} + \frac{1}{m_{ion}}\right)}} \quad (1)$$

   2. Find the drift times (t_D) of the PA calibrants and the ternary complexes by first obtaining the average arrival times (t_A) from the maxima of the corresponding ATD curves and then applying **Equation 2**, where c = detector delay coefficient (1.41 ms; check instrument as this can vary between instruments) and m/z = mass-to-charge ratio of the PA calibrant or amb ternary complex.

$$t_D = t_A^{\frac{c\sqrt{m/z}}{1000}} \quad (2)$$

3. Create a graph by plotting the PA calibrants' t_D vs. Ω_C. Then, using **Equation 3**, fit the data with a least-squares regression to find the constants A' and B, where A' corrects for the electric field, temperature, and pressure in the instrument and B corrects for the nonlinear behavior of the T-wave IM device.

$$\Omega_C = A' t_D^B \quad (3)$$

4. Utilizing the A' and B constants and the t_D value of the amb ternary complexes, calculate their Ω_C using **Equation 3** and their Ω using **Equation 1**. The CCS values estimated by this method have absolute errors of about 2%[29].

7. Computational methods

1. Use the semi-empirical PM6[32] method implemented in structural modeling and computational software[33] to locate geometry-optimized conformers of the [amb +M(II)+NTA]$^-$ ternary complexes and the ion and neutral product pairs: [amb+M(II)]$^-$ + NTA and [NTA+M(II)]$^-$ + amb observed from the CID experiments. Refer to the computation visualizer usage in the **Supplementary File** for specifics on how to develop and submit calculations.
   NOTE: For the present systems, the PM6 method correctly reproduced experimental data, but in general, any quantum chemistry method that is reliable and computationally doable can be used.
2. Run geometry optimizations and frequency calculations on multiple different starting structures to explore different conformations, protonation states, and potential binding sites. Record the electronic + zero-point energies of each of the located stationary points for each of the ternary complexes and their products.
   NOTE: The starting structures for the geometry optimizations should investigate different possible combinations of binding sites and conformational arrangements. The starting structures were based on previously located B3LYP[34] [amb+M(II)]$^-$ conformers[3,4,6]. For [amb+M(II)+NTA]$^-$, NTA was positioned to compete with the substituent sites of the amb at the Aa_1-Aa_2-Aa_6-Aa_7 and the carboxylate terminus for the singlet spin state of Zn(II) or the triplet spin state of Ni(II).
3. Use a program that can perform accurate collision cross-section measurements as measured in helium buffer gas (CCS_{He}) using the atomic coordinates from these quantum chemical calculations[35].
   NOTE: Programs developed for calculating accurate CCS_{He} from peptide structures located by quantum chemical calculations include MobCal[36] and HPCCS[37,38].
4. Choose the lowest energy conformer exhibiting the Lennard-Jones CCS_{He} that agrees with the IM-MS-measured CCS_{He} for selecting the structures of ternary complexes and dissociation products to include in the CRUNCH modeling below.

8. CRUNCH modeling

1. Create a text file in the format described in the discussion section ("CRUNCH input text file format").
   NOTE: The file includes the following columns: (−1) center-of-mass collision energy (E_{cm}), (1) mean of the relative intensity of the [amb+M(II)]$^-$ product, (2) standard deviation of the [amb+M(II)]$^-$ intensity, (3) mean of the

relative intensity of the $[NTA+M(II)]^-$ product, and (4) standard deviation of the $[NTA+M(II)]^-$ intensity.

2. Model the E_{cm}-dependent intensities of the two reaction channels $[amb+M(II)+NTA]^-$ to $[amb+M(II)]^-$ + NTA and $[amb+M(II)+NTA]^-$ to $[NTA+M(II)]^-$ + amb using the TCID technique in the CRUNCH program.

   NOTE: Use the PM6 vibrational and rotational frequencies for the ternary complex and the two ion and neutral product channels. Use average masses of the ternary complex, argon collision gas, and ion and neutral products. Use values from the PM6 calculations or the NIST database for the polarizabilities ($Å^3$) and dipole moments (Debye) for the neutral products.

   1. From the CRUNCH main menu, open the text file (.GB5) containing the E_{cm}-dependent relative intensities of the products. Reply **No** to **read parameters**.

   2. From the CRUNCH main menu, select **Modeling > Set all parameters**. From the reaction model options, choose the default **Threshold CID** option followed by **RRKM with integration over the energy transfer distribution** of the ternary complex[20], enter **2** for **independent product channels modeled**, and select **Calculate cross sections**. Enter **No** to **Do any two product channels have the same ion mass?**

   3. For **Product Channel # 1**, enter column [**1**] for the **experimental data** of the $[amb+M(II)]^-$ product, column [**2**] for the **standard deviations** of the $[amb+M(II)]^-$ product, column [**5**] for the **unconvoluted model cross section**, and column [**6**] for the **convoluted model cross section**. Enter **0** for residuals of fit.

      NOTE: These column numbers correspond to the columns in the input file in step 8.1. as described in the discussion ("CRUNCH input text file format").

   4. For **Product Channel # 2**, enter column [**3**] for the **experimental data** of the $[NTA+M(II)]^-$ product, column [**4**] for the **standard deviations** of the $[NTA+M(II)]^-$ product, column [**7**] for the **unconvoluted model cross section**, and column [**8**] for the **convoluted model cross section**. Enter **0** for residuals of fit.

   5. For the **type of unconvoluted model**, choose **0 K cross section (kinetic shift included)**, which includes the statistical RRKM correction of the kinetic shifts due to the 50 µs time window from the collision cell to the TOF detector[18].

   6. For the **convolution options**, choose **Tiernan's double integral**, which includes the convolution over translational energy distributions between the ternary complex ion and the argon collision gas[21].

   7. For the **numerical integration method**, choose **gaussian quadrature with pre-saved cross sections**, followed by the number of integration points = **32**, the number of standard deviations = **3.0**, and the number of standard deviations for the second integral = **3.0**.

   8. The mass of ternary complex ion (u) is read automatically from the .GB5 text file, followed by the mass of the collision gas (**39.948** for argon); use the defaults of **0.20 eV** for the FWHM of the ion beam and **298.15 K** for gas temperature. The program automatically reads in the **minimum** and **maximum**

center-of-mass collision energies from the .GB5 text file; use the default value for the **minimum energy increment**.

9. Use the default value for the **scaling factor Sig0**, **No** for **allow scaling of individual product channels**, and the default values for **N** and **M**. For the **method for the g(i) calculation**, choose **integrate over ro-vibrational density of states**, which includes the internal energy distribution[20] of the ternary complex [amb+M(II)+NTA]$^-$.

10. From the options for entering the molecular parameters, enter **G** to read the structural modeling file[33] with the PM6 vibrational and rotational frequencies of the ternary complex. Reply **Yes** to the question **is one of the reactants atomic?** Write the location and name of the modeling file.
    NOTE: The other options for entering the vibrational and rotational frequencies include **read parameter file**, which will read in the parameters from a text file, or **edit/enter constants**, which allows for manual entry of each parameter.

11. Scale the frequencies using the NIST-recommended PM6 scaling factor (1.062). For more details on scaling, see the discussion ("scaling factors for the vibrational frequencies"). The number of atoms in the ternary complex is read from the file. Reply **No** to **is the molecule linear?** Enter the **description of the reactants** (e.g., H+Zn+NTA- + Ar).

12. Enter **1** for the **charge on ion** and **1.664** for the **polarizability of the argon gas**[39]. The **mass of ion** and **mass of target** are for the ternary complex and argon, respectively, and are automatically read from the .GB5 text file. Enter **0** for **harmonic vibrations**.
    NOTE: The following options are for choosing different scaling factors for high or low vibrational frequencies. Enter **1.062** for **high frequencies** and **0.0** for **low frequencies** (see discussion: scaling factors for the vibrational frequencies). The scaled frequencies are shown. Choose **0** to select **No Change**.

13. Hit Enter to read the **1-D** and **2-D rotational constants** from the structural modeling file[33] entered in step 8.2.10. Select default values of **0** for the **hindered rotor treatments** and **1** for **molecule symmetry**.
    NOTE: The program shows the inputted data; hit Enter for **No Changes**.

14. Choose the default **300 K** for **reactant temperature**. Select **Integration** for the method for **reduction of density of states array**. Select **Yes** to **truncate the energy distribution**. Enter **40000 cm^{-1}** for **maximum energy for distribution**, **2.0 cm^{-1}** for **bin size**, and **32** for **number of points in energy distribution**.
    NOTE: Hit Enter 2x and check that the **truncated 32-pt array** has a population >0.9. If >0.9, enter **No** to **change bins or condensation factor**. If <0.9, enter **Yes** and change the **maximum energy for distribution** and/or **bin size**.

15. For **parameters for TCID/RRKM model**, choose **Yes** for **Change**, enter **0** for **fixed time**, and **0.000050 s** for the **upper limit of the detection window**. For the utilized instrument, this is the time ions take to travel from the transfer collision cell to the TOF detector and is calculated using **Equation 2**.

16. For **energized molecule**, enter **C** to **copy values** from the reactants already entered. Enter **−1** for source transition state (TS), **0** for destination TS, and **P** to proceed.

17. For **product channel 1**, select **1** for **single transition state** from the **dissociation channel options** and **0** for **none** for the **sequential dissociation**. For the **transition state type**, choose **1** for **orbiting**.

18. Select **G** to read the modeling program files that contain the PM6 rotational and vibrational parameters for the $[amb+M(II)]^-$ + NTA products. Enter **No** for **is one of the PSL TS species atomic?** Enter the location and name of the $[amb+M(II)]^-$ file. Use **1.062** for **scale frequencies**, hit Enter for the number of atoms, and enter **No** for **is the molecule linear?**

19. Enter the location and name of the modeling file that contains the vibrational and rotational frequencies for the NTA product. Use **1.062** for **scale frequencies**, hit Enter for the **number of atoms**, and enter **No** for is the **molecule linear?** Enter the description of the **orbiting TS**, e.g., H+Zn-...NTA.

20. Enter **1** for **charge of** $[amb+M(II)]^-$ **ion**, and enter the **polarizability** (**16.12 Å^3**) and the **dipole moment** (**4.6183 Debye**) of NTA. Select **0 K** for **rotational temperature** and **locked-dipole** for the treatment of the orbiting transition state. Enter the average **masses** (u) of the $[amb+M(II)]^-$ ion and NTA.

21. Enter **0** for **harmonic vibrations**. Enter **1.062** for **high frequencies** and **0.0** for **low frequencies**. See the discussion section for further details of scaling frequencies; the scaled frequencies are shown. Choose **0** to select **No Change**. Hit Enter to read the **1-D** and **2-D rotational constants** from the modeling files. Select **0** for **hindered rotors**, **1** for **molecule symmetry**, and **1** for **reaction degeneracy**. Enter the **No Changes** option.

22. For **product channel 2**, select **1** for **single transition state**, **0** for **none** for the **sequential dissociation**, and **1** for **orbiting** for the **transition state type**.

23. Select **G** to read in modeling files that contain the PM6 rotational and vibrational parameters for the $[NTA+M(II)]^-$ and amb products. Enter **No** for **is one of the PSL TS species atomic?** Write the location and name of the $[NTA+M(II)]^-$ modeling file.

24. Use **1.062** for **scale frequencies**, hit Enter to read the number of atoms, and enter **N** for **is the molecule linear?** Write the location and name of the amb modeling file. Use **1.062** for **scale frequencies**, hit Enter for the number of atoms, and enter **N** for is the **molecule linear?**

25. Enter the description of the **orbiting TS** (e.g., NTA +Zn-...H). Enter **1.0** for **charge** of $[NTA+M(II)]^-$ ion, and enter the **polarizability** (**Å^3**) and the **dipole moment** (Debye) of the amb. Select **0.0** K for **rotational temperature** and **locked-dipole** for the treatment of the orbiting transition state. Enter the average **masses** (u) of the $[NTA+M(II)]^-$ and amb products.

NOTE: The output file contains the polarizability and dipole moments of the amb. The polarizability is in units of Bohr^3 and needs to be converted to the units of Å^3.

26. Enter **0** for **harmonic vibrations**. Enter **1.062** for **high frequencies** and **0** for **low frequencies**. See the discussion for more details on scaling frequencies. The scaled frequencies are shown. Choose 0 to select No Change. Hit Enter to read the **1-D** and **2-D rotational constants** from the modeling files. Select **0** for **hindered rotors**, **1** for **molecule symmetry**, and **1** for **reaction degeneracy**. Enter **No Changes**.

27. To **handle inactive 2-D rotations**, select the default options **statistical angular momentum distribution** and **integrate P(E,J) over J distribution**. Use the default value of **32** in the number of points in integration.

    NOTE: These selections choose the method for integration over the total angular momentum J levels[16, 17]. The resulting output allows the investigator to check that all the input is correct.

28. Select the **activation energies relative to** the **energized molecule** option and enter **relative energy** (eV) for **product channel 1** that is close to the threshold energy observed in the graph of the relative intensity vs. center-of-mass collision energy of the $[amb+M(II)]^-$ product (**Figure 4**).

29. For **product channel 2**, enter **relative energy** (eV) that is close to the threshold energy observed in the graph of the intensity vs. center-of-mass collision energy of the $[NTA+M(II)]^-$ product. To calculate the **number of states** for each product channel, use a bin size of **2.0**. Press Enter and then **No** to continue.

30. From the **Model** menu, select **Optimize parameters to fit data**, and enter the **minimum energy** and **maximum energy** to begin and end the data fit, respectively.

    NOTE: Use a small energy range that includes the thresholds of both channels. For further details, see discussion: energy range for fitting the selected TCID model to the experimental data.

31. Select **-1** for weighting modes **experimental standard deviations**. Based on the data, select a **minimum acceptable std. deviation** of typically 0.01 to 0.001. Select **No** for **optimized scaling of individual channels** and **0** for the **number of iterations**.

    NOTE: An alternative to using standard deviations is the **statistical** option.

32. Use the default value for the **E_0 convergence limit** and select **No** to **hold any parameter at present value**. Enter **0.5** and **2.0** eV for the **lower and upper limits to avoid optimization failure** and **select central finite difference** for the **derivative evaluation method**. Use the default value for **numerical precision** and select **No** for **change derivative step sizes**.

    NOTE: An alternative method is to select **Yes** to **hold any parameter at present value**. This method is described further in the discussion: optimization of parameters.

33. From the **Optimization** menu, select **begin optimization**. The CRUNCH program will optimize the selected TCID model to the experimental data.

    NOTE: If the optimization does not find satisfactory fits, from the **changes** menu, try changing the **energy range** to cover just the first few intensities rising from the thresholds. When a reasonable fit is located, increase the energy range and fit

again. Other options that can help find fits to the data include choosing to **hold any parameter at present value** in **parameters optimized** and changing weighting options in **weights**. See the discussion for these options.

34. When a model fit to the data is found, hit Enter until the **Model** menu appears. If only part of the energy range of experimental data is fitted with the TCID model, select **Calculate and convolute model** to extend the model fit to all experimental collision energies.

35. In the **Model** menu, select **Delta H and S at T**.
NOTE: The unconvoluted CRUNCH model relates the 0 K threshold energies to the 0 K enthalpies (ΔH_0) of dissociation of the ternary complex into the two independent product channels (**Table 2**). The 298 K enthalpies (ΔH_{298}) and Gibbs free energies (ΔG_{298}) of dissociation are also derived with statistical mechanics thermal and entropy corrections using the reactant and products PM6 rotational and vibrational frequencies.

Representative Results

The competitive collision-induced dissociation of the [amb +M(II)+NTA]$^-$ ternary complexes of **A** and **H** into [amb+M(II)]$^-$ + NTA or [NTA+M(II)]$^-$ + amb, are shown in **Figure 3**. The amb is shown as either **A** or **H** and the M = Zn or Ni. The [A +Zn(II)+NTA]$^-$ ternary complex (**Figure 3A**) exhibits apparent thresholds of about 0.7 eV collision energy (CE) to produce [A+Zn(II)]$^-$ and about 0.9 eV to produce [NTA+Zn(II)]$^-$. The dissociation of the [A+Ni(II)+NTA]$^-$ complex (**Figure 3B**) exhibits similar thresholds (~1.1 eV) for both the [NTA+Ni(II)]$^-$ and [A+Ni(II)]$^-$ products, with [NTA+Ni(II)]$^-$ increasing to 90% relative intensity, while the intensities of [A+Ni(II)]$^-$ do not rise above 18%. For the [H+Zn(II)+NTA]$^-$ ternary complex (**Figure 3C**), the main product is [H+Zn(II)]$^-$ rising from a threshold of about 0.6 eV to about 85% relative intensity, and at energies above 1.0 eV, the [NTA+Zn(II)]$^-$ rises to about 30%. There is also a channel for water loss from [H-H_2O+Zn(II)]$^-$. For [H+Ni(II)+NTA]$^-$ (**Figure 3D**), the [H+Ni(II)]$^-$ rises from a threshold of about 0.9 eV to about 40% relative intensity, while the [NTA+Ni(II)]$^-$ rises from ~1.0 eV to about 80%. Included on the graphs is the CE where the ternary complex is 50% dissociated. The Ni(II) ternary complexes require 0.31-0.37 eV higher CE than their Zn(II) ternary complex counterparts to be 50% dissociated. This suggests the Ni(II) complexes are more stable and require higher CE to dissociate, which is further investigated using the TCID technique.

Figure 4 illustrates the competitive TCID method, which allows for the simultaneous fitting of the two competing product channels.

[amb+M(II)+NTA] → [amb+M(II)]$^-$ + NTA (1)

[amb+M(II)+NTA] → [NTA+M(II)]$^-$ + amb (2)

The potential energy surface (PES) illustrates the energized ternary complex dissociating into the competing product channels and shows the PM6 geometry-optimized species used to model the dissociation of [amb$_H$+Zn(II)+NTA]$^-$. Included in the PES are the density of states of the ternary complex and the sum of states of the products. The 0 K threshold energies, E_1 and E_2, equate to the 0 K enthalpy change for reactions 1 and 2.

Figure 5 shows the structures of the other three geometry-optimized ternary complexes used in this study. These species were chosen based on their predicted electronic and zero-point energies and their agreement with the IM-MS-measured collision cross-sections (CCS_{He}). **Table 1** shows

there is an agreement between the ternary complexes LJ CCS_{He} and the experimental IM-MS CCS_{He} because they agree within their mutual uncertainties. The conformations of the [amb+M(II)] and amb were based on the findings of our previous DFT modeling[3,4,5,6]. The molecular parameters of these PM6 conformers were used in the TCID modeling of the energy-resolved dissociations of the ternary complexes, including their ro-vibrational frequencies for calculating their density and sum of states.

Figure 6 shows the convoluted CRUNCH TCID threshold fits to the energy-resolved product intensities. The convoluted fits include the available energy and angular momentum distributions of the $[amb+M(II)+NTA]^-$ + Ar reactants. The unconvoluted fits (not shown) predicted the 0 K change in enthalpies (ΔH_0) for the dissociation of the ternary complex, and **Table 2** shows the ΔH_0 and ΔH_{298} (kJ/mol) for reactions 1 and 2. For the dissociation of the Zn(II) ternary complexes, both **A** and **H** exhibit ΔH_0 for reaction 1, which are 31 kJ/mol and 15 kJ/mol lower than the ΔH_0 for reaction 2, respectively, indicating both **A** and **H** have greater Zn(II) affinity than the NTA. The $[A+Ni(II)+NTA]^-$ ternary complex exhibits ΔH_0 = 146 and 148 kJ/mol for reactions 1 and 2, respectively, indicating **A** and NTA have similar affinities for Ni(II). However, the dissociation of $[H+Ni(II)+NTA]^-$ shows the ΔH_0 for reaction 1 is 36 kJ/mol lower than for reaction 2, indicating **H** has a greater Ni(II) affinity than the NTA. Overall, the $[amb+Ni(II)+NTA]^-$ complexes exhibit higher dissociation enthalpies than their $[amb+Zn(II)+NTA]^-$ counterparts, with the exception of **A** dissociating into $[NTA+Ni(II)]^-$. **Table 3** shows the Gibbs free energies (ΔG_{298}) of association and the formation constants (K) for the reverse reactions:

$$[amb+M(II)]^- + NTA \rightarrow [amb+M(II)+NTA]^- \quad (3)$$

$$[NTA+M(II)]^- + amb \rightarrow [amb+M(II)+NTA]^- \quad (4)$$

Table 3 demonstrates that the formation of the Ni(II) ternary complexes is more exergonic and exhibits larger formation constants K than the Zn(II) complexes in all cases. Reaction 4 (i.e., the amb tag association with the NTA metal ion complex) is of particular interest as it represents the amb-tagged recombinant protein binding to the NTA-immobilized metal ion inside the IMAC column. Reaction 4 for the formation of $[amb_A+Ni(II)+NTA]$ exhibits the most spontaneous ΔG_{298} = 53.1 kJ/mol and the highest formation constant, K = 2.01 x 10^9.

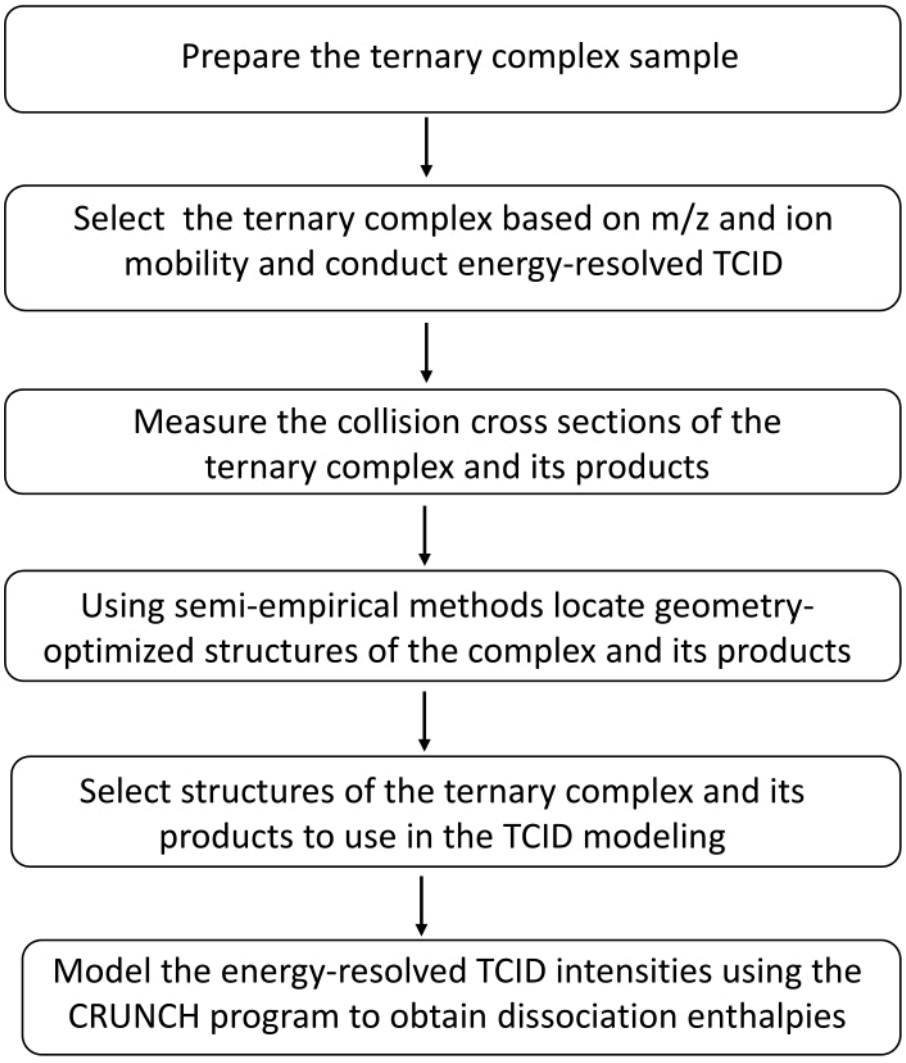

Figure 1: Overview of the ES-IM-MS TCID method. Please click here to view a larger version of this figure.

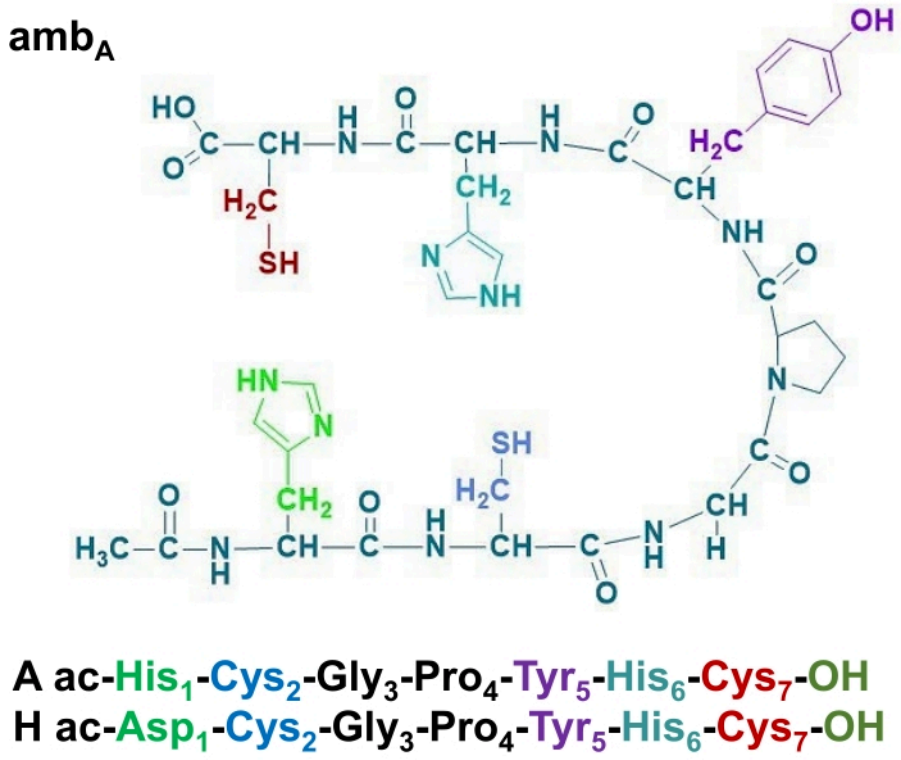

Figure 2: The primary structures of amb A and H peptides. Color highlights the potential metal-binding sites. Please click here to view a larger version of this figure.

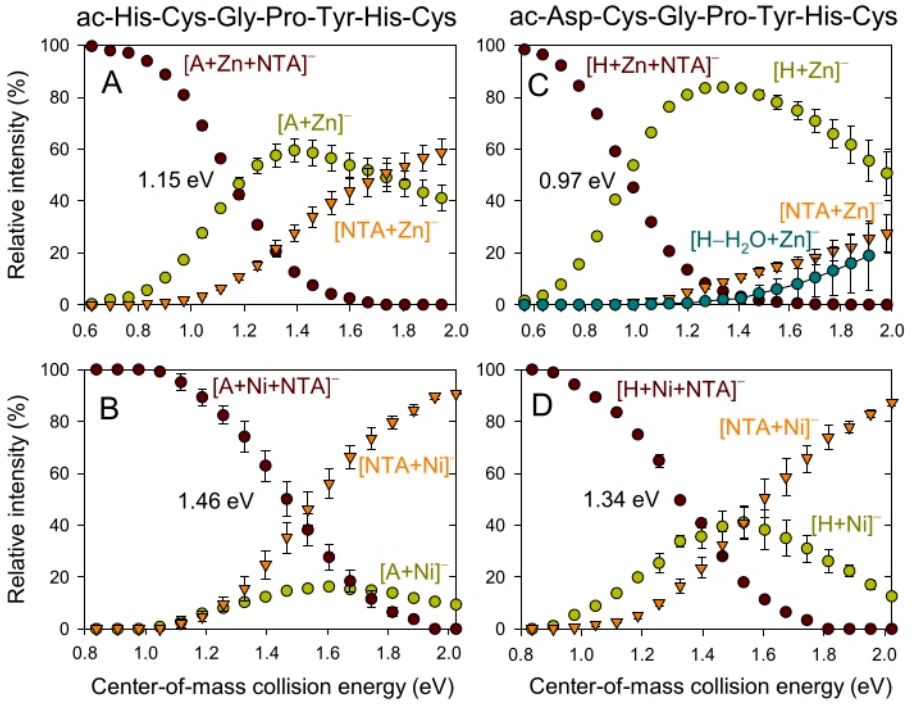

Figure 3: The center-of-mass, energy-resolved (eV) threshold collision-induced dissociation of [amb+M(II)+NTA]⁻. The energy-dependence of the product ions [amb+M(II)]⁻ [NTA+M(II)]⁻ and [amb-H_2O+Zn(II)]⁻ is shown. The center-of-mass collision energy, where there is 50% dissociation of the [amb+M(II)+NTA]⁻ ternary complex, is included on the graphs.

Please click here to view a larger version of this figure.

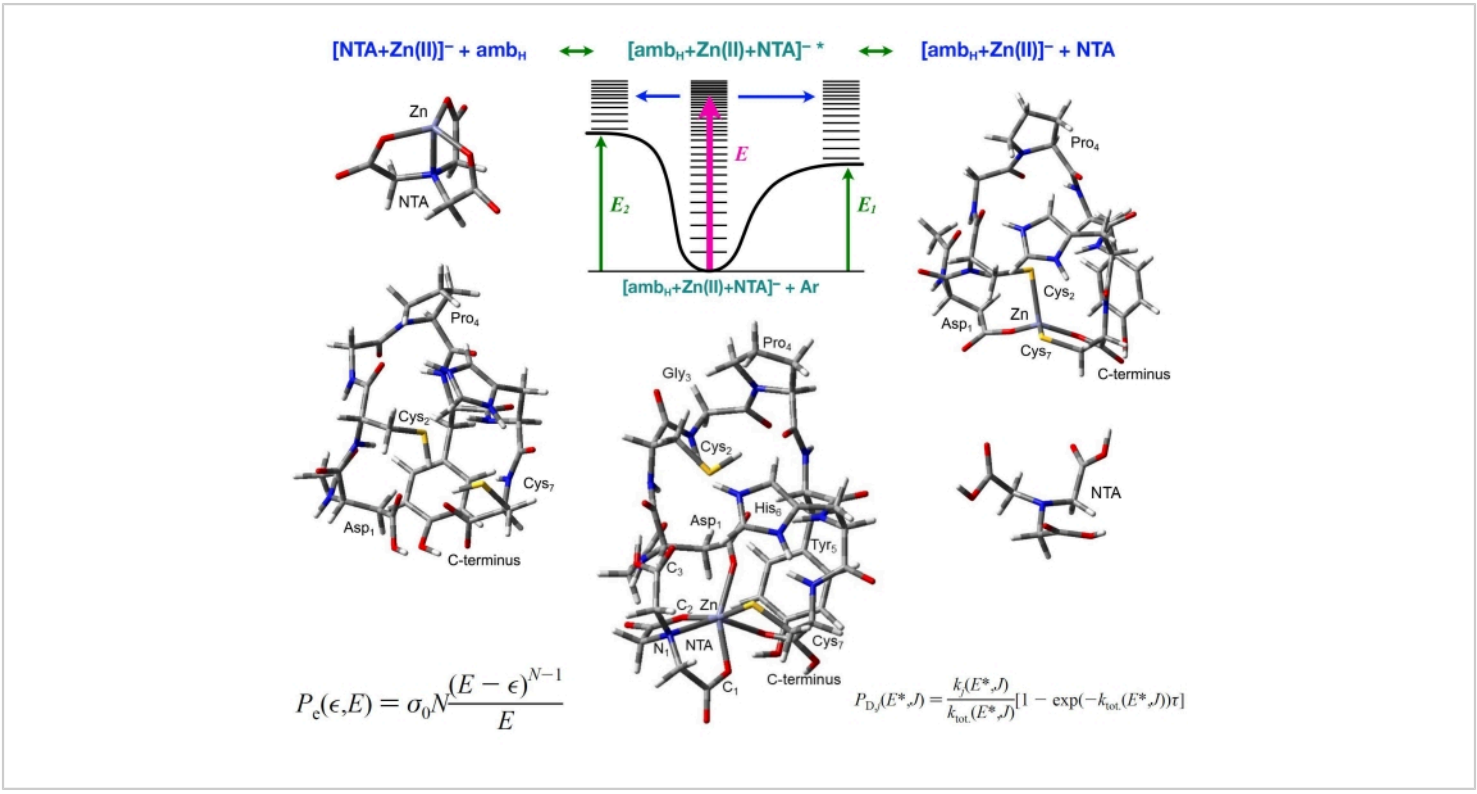

Figure 4: The model for the energy-resolved TCID method. The collisions between $[amb_H+Zn(II)+NTA]^-$ + argon result in the dissociation to the $[amb_H+Zn(II)]^-$ + NTA or $[NTA+Zn(II)]^-$ + amb_H products. The threshold energies E_1 and E_2 equate to the 0 K enthalpies of dissociation (ΔH_0) for the reactions $[amb_H+Zn(II)+NTA]^- \rightarrow [amb_H+Zn(II)]^-$ + NTA or $[amb_H+Zn(II)+NTA]^- \rightarrow [NTA+Zn(II)]^-$ + amb_H, respectively. Please click here to view a larger version of this figure.

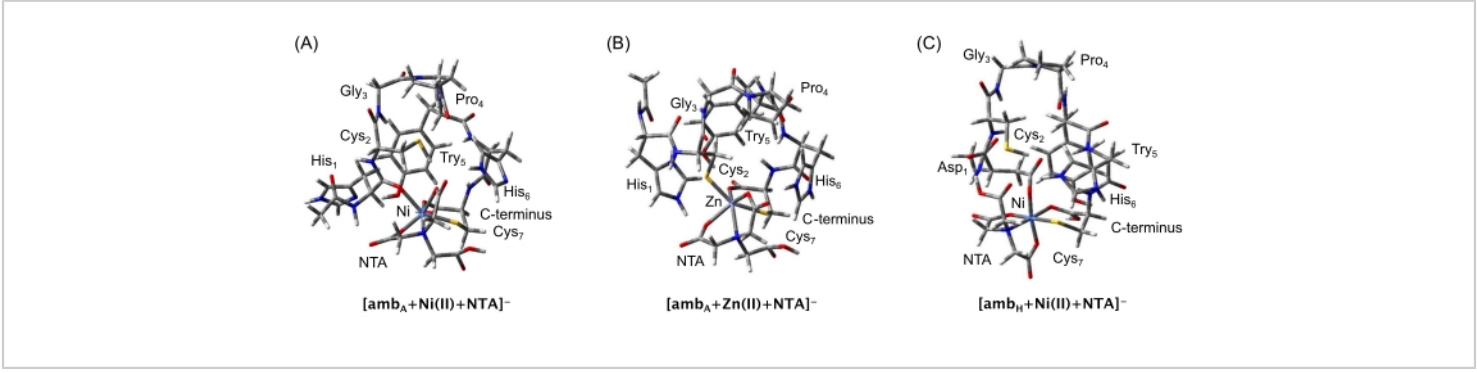

Figure 5: The PM6 geometry-optimized ternary [amb+M(II)+NTA]⁻ complexes of A and H. Conformers used in the TCID modeling of the experimental data. These conformers were selected from other candidate structures by comparing their PM6 electronic energies and how their LJ collision cross-sections (CCS_{He}) compared to the IM-MS measured CCS_{He}. Please click here to view a larger version of this figure.

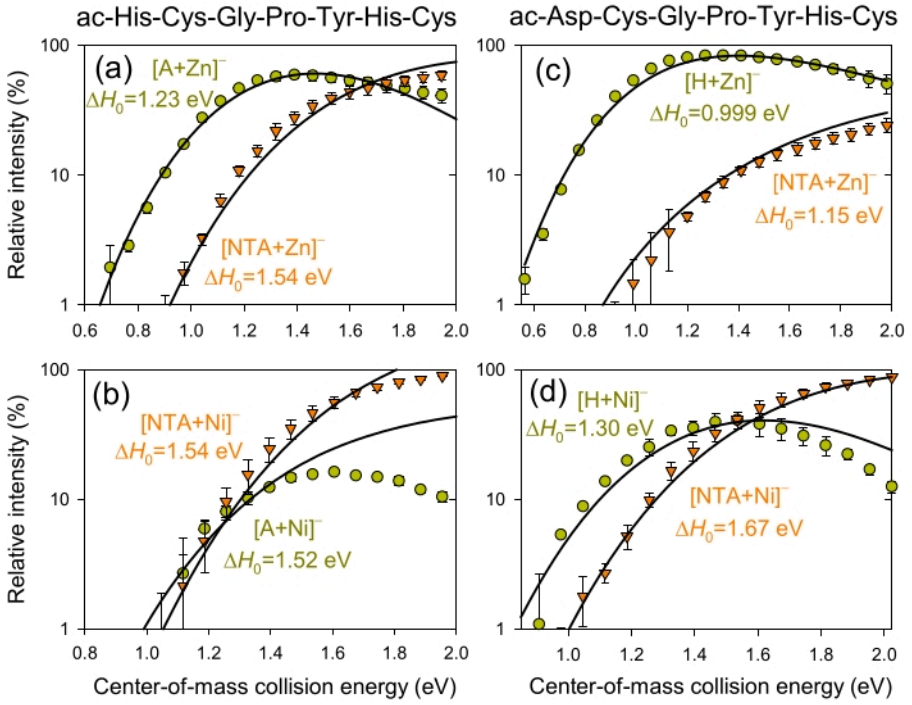

Figure 6: The energy-resolved, collision-induced dissociation of [amb+M(II)+NTA]⁻. For species A and H, the product ions of [amb+M(II)]⁻ and [NTA+M(II)]⁻ with the convoluted CRUNCH threshold fits are shown. The energy (eV) values shown are the enthalpies of dissociation at 0 K for the reactions [amb+M(II)+NTA]⁻ → [amb+M(II)]⁻ + NTA or [amb+M(II)+NTA]⁻ → [NTA+M(II)]⁻ + amb. Please click here to view a larger version of this figure.

Figure 7: The format for the CRUNCH text input file. The file contains the mean relative intensities and their standard deviations of the product ions formed as a function of center-of-mass collision energy. Please click here to view a larger version of this figure.

amb	[amb+Zn(II)+NTA]$^-$		[amb+Ni(II)+NTA]$^-$	
	PM6	Exp.[a]	PM6	Exp.[a]
A	214±2	214	219±2	218
H	211±5	216	212±3	215
[a] ES-IM-MS CCS_{He} measurements have uncertainties of ±4 Å^2.				

Table 1: Comparison of LJ collision cross-sections of the PM6 conformers of [amb+M(II)+NTA]$^-$. Theoretical cross-sections of the PM6 conformers are compared with the experimental CCS_{He} measured with ES-IM-MS.

	[amb+Zn(II)+NTA]$^-$ →				[amb+Ni(II)+NTA]$^-$ →			
	[amb+Zn(II)]$^-$ + NTA		[NTA+Zn(II)]$^-$ + amb		[amb+Ni(II)]$^-$ + NTA		[NTA+Ni(II)]$^-$ + amb	
amb	ΔH_0	ΔH_{298}	ΔH_0	ΔH_{298}	ΔH_0	ΔH_{298}	ΔH_0	ΔH_{298}
A	118	127	149	182	146	171	148	154
H	96.4	92.3	111	115	125	140	161	216

Table 2: Thermochemical results from the TCID analyses. The energy-dependent reactions [amb+M(II)+NTA]$^-$ → [amb +M(II)]$^-$ + NTA or [amb+M(II)+NTA]$^-$ → [NTA+M(II)]$^-$ + amb, showing the 0 K enthalpies of dissociation (ΔH_0) derived from the unconvoluted TCID model fit, and 298 K enthalpies of dissociation (ΔH_{298}) derived from ΔH_0 and statistical mechanics thermal corrections using the PM6 rotational and vibrational frequencies. Values are given in kJ/mol.

	[amb+Zn(II)]$^-$ + NTA →		[NTA+Zn(II)]$^-$ + amb →		[amb+Ni(II)]$^-$ + NTA →		[NTA+Ni(II)]$^-$ + amb →	
	[amb+Zn(II)+NTA]$^-$		[amb+Zn(II)+NTA]$^-$		[amb+Ni(II)+NTA]$^-$		[amb+Ni(II)+NTA]$^-$	
amb	ΔG_{298}	*K*	ΔG_{298}	*K*	ΔG_{298}	*K*	ΔG_{298}	*K*
A	-34.0	9.05×10^5	-21.8	6.59×10^3	-45.7	1.01×10^8	-53.1	2.01×10^9
H	-29.3	1.36×10^5	-30.2	1.95×10^5	-47.0	1.71×10^8	-31.1	2.81×10^5

Table 3: Gibbs free energies of association (ΔG_{298}) and equilibrium formation constants (*K*). ΔG_{298} and *K* at 298 K for the reverse reactions [amb+M(II)]$^-$ + NTA → [amb+M(II)+NTA]$^-$ and [NTA+M(II)]$^-$ + amb → [amb+M(II)+NTA]$^-$. Derived from ΔH_{298} and statistical mechanics entropy calculations using the PM6 rotational and vibrational frequencies. Values for ΔG_{298} are in kJ/mol.

Supplementary File. Please click here to download this File.

Discussion

Critical steps

ES-IM-MS threshold collision-induced dissociation (TCID) analyses. The TCID used the transfer T-wave cell in the presence of argon as the collision cell. Prior to dissociation, the precursor ions are thermalized by low-energy collisions with nitrogen gas as they pass through the ion mobility (IM) cell. This results in a more reproducible energy-resolved TCID than is achieved by using the trap as the collision cell[6,40]. The thermalization of the [amb +M(II)+NTA]$^-$ prior to dissociation also allows the available internal energy of the ternary complex to be characterized using 298 K temperature. The dissociation in the transfer cell also means the ternary complex and its product ions have the same average arrival times at the detector, which was useful for identifying the dissociation of the ternary complex that only occurred in the transfer cell. Other regions where dissociation can occur are the ES source (sampling cone is kept at 25 V to avoid this) or at the entrance of the IM cell. The product ions produced by the dissociation of the ternary complex in these regions have different drift times from those produced in the transfer cell because the product ions are separated from the ternary complex in the IM cell. Those product ions were excluded from the analysis. In this protocol, only the integrated arrival time distributions for the precursor and product ions that are co-aligned are used to determine their intensities. The trap bias setting is the voltage that controls the injection voltage into the IM cell, which contributes to the CID at the entrance of the IM cell. The trap bias was set at 14 V, which kept the background dissociation to a minimum while not overly affecting the overall intensities. A previous study[41] determined the effective temperature (upper limit) of the peptide dimer of leucine enkephalin to be 449 K at the entrance of the IM cell. However, the effective temperature decreased rapidly as the dimer passed down the IM cell. The arrival times of the amb complexes studied here exhibited Gaussian distributions, indicating they were thermalized as they passed down the IM cell.

ES-IM-MS collision cross sections (CCS) analyses. CCS drift times were found experimentally as the result of collisions with nitrogen. Those values were converted to helium-derived CCS drift times using a calibration curve of known standards. This is essential as the programs used to measure the CCS of the PM6 conformers require the more commonly used helium standards.

Modifications and troubleshooting of the technique

CRUNCH input text file format. The input text file suitable for the CRUNCH program is shown in **Figure 7**. The headers in order from top to bottom are file location and version of CRUNCH; date; number of energies; number of data series excluding the first energies column; source file; mass of the precursor complex; mass of argon; temperature of experiment; date of creation; x-data designated as −1 (the center-of-mass collision energies); and the full width at half maximum (FWHM) of the ion beam. These values must be modified for each TCID experiment. The FWHM energy spread of the ion beam and energy zero should be determined by retarding potential analysis (RPA) by scanning the CE through low voltages and monitoring the total ion current. However, under the operating conditions of the IM in the current study, the ion current signal only decreased by about 50% when the transfer CE was set to its lowest value. The ion beam energy zero and FWHM could be measured only upon additional retardation by lowering the exit IM lens. In this latter case, the FWHM of the derivative of the RPA curve gave a typical ion energy spread of 1.5 V in the lab-frame or 0.035 eV in the center-of-mass frame[13].

The pressures row relates to pressure inside the collision cell but is not used here. The pressures of argon in the collision cell can be varied and the TCID data can be measured at three pressures to extrapolate to single collision conditions. However, only one pressure was used in this study, and the pressure results in multiple collisions. Developing the new platform for a single collision is an area of ongoing research. Masses relate to the two product ions whose intensities are in the columns below. Dwells can be left as default. The five columns are the center-of-mass collision energies (designated −1); the mean of the ion intensities of the species with mass 898.30 u; the standard deviations of the ion intensities of species 898.30 u; the mean of the ion intensities of the species with mass 253.53 u; and the standard deviations of the ion intensities of species 253.53 u.

Molecular Modeling

The number of conformers were narrowed initially by using models derived from previous studies[9,10,11,12,13]. CRUNCH fitting requires careful screening of reactants, activated molecules, and transition states to obtain accurate threshold energies. Previous research[9,10,11,12,13] has included extensive screening of [amb+M(II)] conformers to obtain the structures with the parameters used in the CRUNCH modeling here. Only complexes with *trans* peptide bonds were used because only they are in agreement with IM-MS measured CCS_{He}[10]. The B3LYP and PM6 molecular modeling methods both predict the lowest energy $[amb+M(II)]^-$ conformer that exhibits Aa_1-Cys_2-Cys_7 and carboxylate terminus coordination of Zn(II) or Ni(II)[10,11,12,13]. Familiarity with the behaviors of the known models allowed for the new conformers of $[amb+M(II)+NTA]^-$ to be determined more efficiently. To assist in conformer determination, as lower energy conformers were located by the PM6 method, they were filtered out and reassessed systematically until the most feasible, lowest energy conformers remained.

CRUNCH modeling

Time-window for observing dissociation. In this study, the 50 µs time window from the beginning of the transfer cell to the end of the TOF analyzer, where the multichannel plate detector is positioned, was used. It may be better to use the experimental time window between activation in the transfer cell and the entrance to the TOF mass analyzer because, if the activated ion dissociates during its time in the reflectron TOF, this metastable decay will be measured at a different *m/z*. However, in this study, the product ions observed in the mass spectra were all identifiable as the unmodified *m/z* species shown in **Figure 3**. This indicates that metastable decay was not an issue. Further research could investigate this by examining a known reaction with a high threshold and checking that the correct threshold energy is obtained using the 50 µs time window and RRKM modelling.

Scaling factors for the vibrational frequencies. The NIST-recommended scaling factors for PM6 (1.062) vibrational frequencies were used. These were satisfactory for fitting the $[A+Zn(II)+NTA]^-$, $[A+Ni(II)+NTA]^-$, and $[H+Zn(II)+NTA]^-$ data. For some cases where the higher energy channel is entropically favored over the lower energy channel, it may be necessary to additionally scale the frequencies of the second channel. One approach is to scale the frequencies below 900 cm^{-1} (as these are the least accurate) to loosen the frequencies and make the TS more entropically favored.

Optimization of parameters. Using the **Yes** option to **Hold any parameter at present value** can be helpful to fit the data successfully. For the first fit, the $E_0(2)$ is held and the model TCID is fitted to the data by optimizing the CONST, $E_0(1)$, and N variables. Once a good fit is located, the **parameters** option and **Hold any parameter at present value** can be used to hold CONST, $E_0(1)$, and N, while allowing $E_0(2)$ to optimize to the data. Finally, once $E_0(2)$ is optimized, in the **parameters** option, all four parameters CONST, $E_0(1)$, $E_0(2)$, and N should be allowed to optimize to the data.

Energy range for fitting the selected TCID model to the experimental data. The energy range used to fit the experimental data should reproduce as much of the experimental intensity data as possible while maintaining a good fit in the threshold region. One can start by fitting the TCID model to a small energy range at the thresholds of the experimental data. One can choose a starting energy that exhibits the background intensity just prior to the rising intensity threshold behavior. Once the TCID fit is optimized to the experimental data range, the range should be increased by 0.1 eV and the fit should be optimized again. This procedure should be repeated to fit as much of the data range as possible while maintaining the fit of the threshold region.

Thermochemical Analyses. The thermochemical results from **Delta H and S at T** option should be compared with a series of different energy range fits to the data to estimate the standard deviation of the TCID model fit. Fits to compare should include smaller ranges that fit the initial rising threshold intensities well with those with greater ranges that include the higher energies as well.

Disclosures

The authors have no conflict of interest to disclose.

Acknowledgments

This material is based upon work supported by the National Science Foundation under 1764436, NSF REU program (CHE-1659852), NSF instrument support (MRI-0821247), Physics and Astronomy Scholarship for Success (PASS) NSF project (1643567), Welch Foundation (T-0014), and computing resources from the Department of Energy (TX-

W-20090427-0004-50) and L3 Communications. The authors thank Kent M. Ervin (University of Nevada - Reno) and Peter B. Armentrout (University of Utah) for sharing the CRUNCH program and for advice on fitting from PBA. The authors thank Michael T. Bower's group at the University of California - Santa Barbara for sharing the Sigma program.

References

1. Kim, Y. -M., Chen, P. Ligand binding energy in [(bipy)Rh(PCH)]+ by collision-induced dissociation threshold measurements. *International Journal of Mass Spectrometry.* **202** (1-3), 1-7 (2000).
2. Plattner, D. Electrospray mass spectrometry beyond analytical chemistry: Studies of organometallic catalysis in the gas phase. *International Journal of Mass Spectrometry.* **207** (3), 125-144 (2001).
3. Narancic, S., Bach, A., Chen, P. Simple fitting of energy-resolved reactive cross sections in threshold collision-induced dissociation (T-CID) experiments. *Journal of Physical Chemistry A.* **111** (30), 7006-7013 (2007).
4. Ervin, K., Armentrout., P. B., Systematic and random errors in ion affinities and activation entropies from the extended kinetic method. *Journal of Mass Spectrometry.* **39** (9), 1004-1015 (2004).
5. Cooks, R. G., Wong, P. S. H., Kinetic method of making thermochemical determinations: Advances and applications. *Accounts of Chemical Research.* **31** (7), 379-386 (1998).
6. Ervin, K., Microcanonical analysis of the kinetic method. The meaning of the "apparent entropy". *Journal of the American Society of Mass Spectrometry.* **13** (5), 435-452 (2002).
7. Amarasinghe, C., Jin, J.-P. The use of affinity tags to overcome obstacles in recombinant protein expression and purification. *Protein & Peptide Letters.* **22** (10), 885-892 (2015).
8. Bornhorst, J. A., Falke, J. J. Purification of proteins using polyhistidine affinity tags. *Methods in Enzymology.* **326**, 245-254 (2000).
9. Yousef, E. N., Angel, L. A. Comparison of the pH-dependent formation of His and Cys heptapeptide complexes of nickel(II), copper(II), and zinc(II) as determined by ion mobility-mass spectrometry. *Journal of Mass Spectrometry.* **55** (3), e4489 (2020).
10. Lin, Y.-F. et al. Weak acid-base interactions of histidine and cysteine affect the charge states, tertiary structure, and Zn(II)-binding of heptapeptides. *Journal of the American Society of Mass Spectrometry.* **30**, 2068-2081 (2019).
11. Wagoner, S. M. et al. The multiple conformational charge states of zinc(II) coordination by 2His-2Cys oligopeptide investigated by ion mobility - mass spectrometry, density functional theory and theoretical collision cross sections. *Journal of Mass Spectrometry.* **51** (12), 1120-1129 (2016).
12. Flores, A. A. et al. Formation of Co(II), Ni(II), Zn(II) complexes of alternative metal binding heptapeptides and nitrilotriacetic acid: Discovering new potential affinity tags. *International Journal of Mass Spectrometry.* **463**, 116554 (2021).
13. Flores, A. A. et al. Thermochemical and conformational studies of Ni(II) and Zn(II) ternary complexes of alternative metal binding peptides with nitrilotriacetic acid. *International Journal of Mass Spectrometry.* **473**, 116792 (2022).

14. Sesham, R. et al. The pH dependent Cu(II) and Zn(II) binding behavior of an analog methanobactin peptide. *European Journal of Mass Spectrometry.* **19** (6), 463-473 (2013).
15. Choi, D. et al. Redox activity and multiple copper(I) coordination of 2His-2Cys oligopeptide. *Journal of Mass Spectrometry.* **. 50** (2), 316-325 (2015).
16. Vytla, Y., Angel, L. A. Applying ion mobility-mass spectrometry techniques for explicitly identifying the products of Cu(II) reactions of 2His-2Cys motif peptides. *Analytical Chemistry.* **88** (22), 10925-10932 (2016).
17. Yousef, E. N. et al. Ion mobility-mass spectrometry techniques for determining the structure and mechanisms of metal ion recognition and redox activity of metal binding oligopeptides. *Journal of Visualized Experiments.* (151), e60102 (2019).
18. Ilesanmi, A. B., Moore, T. C., Angel, L. A. pH dependent chelation study of Zn(II) and Ni(II) by a series of hexapeptides using electrospray ionization - Ion mobility - Mass spectrometry. *International Journal of Mass Spectrometry.* **455**, 116369 (2020).
19. Armentrout, P. B., Ervin, K. M., Rodgers, M. T. Statistical rate theory and kinetic energy-resolved ion chemistry: Theory and applications. *Journal of Physical Chemistry A.* **112** (41), 10071-10085 (2008).
20. Dalleska, N. F., Honma, K., Sunderlin, L. S., Armentrout, P. B. Solvation of transition metal ions by water. Sequential binding energies of M+(H2O)x (x = 1-4) for M = Ti to Cu determined by collision-induced dissociation. *Journal of the American Chemical Society.* **116** (8), 3519-3528 (1994).
21. Ervin, K. M., Armentrout, P. B. Translational energy dependence of $Ar^+ + XY \rightarrow ArX^+ + Y$ (XY = H2,D2,HD) from thermal to 30 eV c.m. *Journal of Chemical Physics.* **83**, 166-189 (1985).
22. DeTuri, V. F., Ervin, K. M. Competitive threshold collision-induced dissociation: Gas-phase acidities and bond dissociation energies for a series of alcohols. *Journal of Physical Chemistry A.* **103** (35), 6911-6920 (1999).
23. Iceman, C., Armentrout, P. B. Collision-induced dissociation and theoretical studies of K+ complexes with ammonia: a test of theory for potassium ions. *International Journal of Mass Spectrometry.* **222** (1-3), 329-349 (2003).
24. Rodgers, M. T., Ervin, K. M., Armentrout, P. B. Statistical modeling of collision-induced dissociation thresholds. *Journal of Chemical Physics.* **106**, 4499-4508 (1997).
25. Rodgers, M. T., Armentrout, P.B. Statistical modeling of competitive threshold collision-induced dissociation. *Journal of Chemical Physics.* **109**, 1787-1800 (1998).
26. Armentrout, P. B., Ervin, K. M. *CRUNCH, Fortran program, version 5.2002.* (2016).
27. Pringle, S. D. et al. An investigation of the mobility separation of some peptide and protein ions using a new hybrid quadrupole/travelling wave IMS/oa-ToF instrument. *International Journal of Mass Spectrometry.* **261** (1), 1-12 (2007).
28. Smith, D. P. et al. Deciphering drift time measurements from travelling wave ion mobility spectrometry-mass spectrometry studies. *European Journal of Mass Spectrometry.* **15** (2), 113-130 (2009).

29. Forsythe, J. G. et al. Collision cross section calibrants for negative ion mode traveling wave ion mobility-mass spectrometry. *Analyst.* **140** (20), 6853-6861 (2015).
30. Allen, S. J., Giles, K., Gilbert, T., Bush, M. F. Ion mobility mass spectrometry of peptide, protein, and protein complex ions using a radio-frequency confining drift cell. *Analyst.* **141** (3), 884-891 (2016).
31. Salbo, R. et al. Traveling-wave ion mobility mass spectrometry of protein complexes: accurate calibrated collision cross-sections of human insulin oligomers. *Rapid Communications in Mass Spectrometry.* **26** (10), 1181-1193 (2012).
32. Stewart, J. J. P. Optimization of parameters for semiempirical methods V: Modification of NDDO approximations and application to 70 elements. *Journal of Molecular Modeling.* **13**, 1173-1213 (2007).
33. Frisch, M. J. et al. *Gaussian 09, Revision C.01.* Wallingford CT: Gaussian, Inc (2012).
34. Becke, A. D. Density-functional thermochemistry. III. The role of exact exchange. *Journal of Chemical Physics.* **98**, 5648-5652 (1993).
35. Wyttenbach, T., von Helden, G., Batka, J. J., Jr., Carlat, D., Bowers, M. T. Effect of the long-range potential on ion mobility measurements. *Journal of the American Society of Mass Spectrometry.* **8**, 275-282 (1997).
36. Shvartsburg, A. A., Jarrold, M. F. An exact hard-spheres scattering model for the mobilities of polyatomic ions. *Chemical Physics Letters.* **261** (1-2), 86-91 (1996).
37. Heerdt, G., Zanotto, L., Souza, P. C. T., Araujo, G., Skaf, M. S. Collision cross section calculations using HPCCS. *Methods in Molecular Biology.* **2084**, 297-310 (2020).
38. Zanotto, L., Heerdt, G., Souza, P. C. T., Araujo, G., Skaf, M. S. High performance collision cross section calculation-HPCCS. *Journal of Computational Chemistry.* **39** (21), 1675-1681 (2018).
39. *https://cccbdb.nist.gov/pollistx.asp.* (2022).
40. Raja, U. K. B., Injeti, S., Culver, T., McCabe, J. W., Angel, L. A. Probing the stability of insulin oligomers using electrospray ionization ion mobility mass spectrometry. *European Journal of Mass Spectrometry.* **21** (6), 759-774 (2015).
41. Merenbloom, S. I., Flick, T. G., Williams, E. R. How hot are your ions in TWAVE ion mobility spectrometry? *Journal of the American Society of Mass Spectrometry.* **23** (3), 553-562 (2012).